the society for solid-state and electrochemical science and technology

Journal of The Electrochemical Society

Tuning Optical Properties of Photonic Crystal of Anodic Alumina and the Influence of Electrodeposition

X. Hu, Z. Y. Ling, T. L. Sun and X. H. He

J. Electrochem. Soc. 2009, Volume 156, Issue 11, Pages D521-D524.
doi: 10.1149/1.3223992

0013-4651/2009/156(11)/D521/4/$25.00 © The Electrochemical Society

Tuning Optical Properties of Photonic Crystal of Anodic Alumina and the Influence of Electrodeposition

X. Hu,[z] Z. Y. Ling, T. L. Sun, and X. H. He

Department of Electronic Materials Science and Engineering, South China University of Technology, Guangzhou 510640, China

In this paper, the tuning optical properties in a photonic crystal of an anodic alumina were investigated together with the influence of the metal electrodeposition on the photonic crystal with an Al substrate. The transmission spectra of the photonic crystal show the redshift of the transmission dip with increasing anodic voltage and the blueshift of the color with observable angles obeying the Bragg law. The electrodeposited metal layer strongly absorbs the reflecting light from the Al substrate, and it makes the photonic crystals with an Al substrate show vivid colors.
 [DOI: 10.1149/1.3223992]

Manuscript submitted July 6, 2009; revised manuscript received August 17, 2009. Published October 1, 2009.

Photonic crystals have been the focus of many researchers over the past two decades because of their applications ranging from optical communications to chemical and biological sensors.[1,2] The fabrication of photonic crystal structures operating at visible and near-infrared wavelengths is a challenging task for nanotechnology research. The numerous nanofabrication strategies being pursued to fabricate photonic crystals include mainly two categories: microlithography and self-assembly.[3] However, sophisticated equipment is required for microlithography, and the self-assembly method has limitations such as difficulty in engineering precise defects.[4]

The photonic bandgap in anodic aluminum oxide was first observed by Masuda et al.[5] in 1999. Wang et al.[6] fabricated a photonic crystal in anodic alumina by adjusting the anodizing cell voltage periodically in the process of electrochemical oxidation and following chemical etching. Lee et al.[7] reported an approach termed "pulse anodization" comprising the mild and hard anodization processes to get a periodical structure. More recently, Losic and Losic[8] fabricated three-dimensional periodical porous structures by combining the cyclic anodization approach and chemical etching.

In the industrial application, anodic oxide on aluminum can be colored by various methods such as electrolytic coloring.[9] In electrolytic coloring, small particles of metal are deposited at the bottom of the pores of the oxide film. Chen et al.[10] reported that the color tuning in thin films of nickel nanowires grown inside an anodic alumina oxide template obeys the rule of interference. The photonic crystal of porous alumina has great potential for the coloring of anodized aluminum[11] for practical application. But, the color cannot be obtained from the photonic crystal with an Al substrate because of the strong light reflection from the interface between the oxide film and the Al.

In the present work, the tuning of optical characterization was obtained by adjusting the function of anodization voltage, and the aluminum was colored for photonic crystal of anodized alumina by metal electrodeposition.

Experimental

For the synthesis of a porous alumina membrane, high purity aluminum sheets (99.99%) were degreased in acetone and alcohol separately, and then the sample was electropolished in a mixture of C_2H_5OH and $HClO_4$ (ratio by volume was 4:1) to smooth the surface. Anodization was conducted in 0.3 M $H_2C_2O_4$ solution at 30°C under a periodic cell for 267 min. Finally, the voltage was lowered stepwise down to 3 V to thin the bottom barrier layer. The general porous alumina was conducted under 40 V for 2 h at 30°C. Electrodeposition was carried out with a constant current density (0.5 mA/cm^2) (1 min for photonic crystal and 3 min for general porous alumina). The electrolyte used to deposit had the following composition: 30–50 g/L $NiSO_4$, 10–15 g/L $SnSO_4$, 20–25 g/L H_2SO_4, 4–6 g/L citric acid, and 15–25 g/L thiourea. The residual aluminum on the back side was removed by immersing it into a saturated $CuCl_2$ solution. The morphology of the membranes was examined with an LEO1530VP field-emission scanning electron microscope. The optical characteristics were measured with a spectrophotometer (TU-1901), and the reflection spectra were performed under a 5° incident angle. The optical images were characterized by an optical digital camera.

Results and Discussion

Anodization was conducted under a periodic cell voltage, as shown in Fig. 1a. The cell voltage decreases linearly from $U_1(U_0 + 10\ \text{V})$ to $U_2(U_0 - 10\ \text{V})$ in 40 s followed by a steady state at U_2 for 30 s, and then it increases sinusoidally from U_2 to U_1 in 10 s. Here, U_0 is defined to be a benchmark anodic voltage. The color is expected to be brighter for the broader reflection peak, which is obtained by adjusting the anodization voltage. Therefore, 1 V is reduced for U_0 after 200 periods, as shown in Fig. 1b. Samples 1#–7# correspond to the initial benchmark anodic voltages (U_0) of 39, 38, 37, 36, 35, 34, and 33 V. The characteristics of the current density time can be explained by the change in the voltage and the thickness of the barrier, which is determined by the thinning of the field-assisted dissolution; the film growth and the details for the characteristics are reported in Ref. 12. The sketch map of the microstructure of the photonic crystal is also shown in Fig. 1c. The microstructures shown in Fig. 2 are observed in the middle of the fracture surface. To get statistically significant data on the distance between the branched channels, 10 periodicities were calculated. As shown in Fig. 2, the average distances between the branched channels of 2#, 3#, 5#, and 7# are 226, 215, 184, and 157 nm. The distance between the branched channels is controlled by adjusting the initial benchmark anodic voltage (U_0).

The transmission spectra for the film are shown in Fig. 3a. In the present work, photonic crystals of anodized alumina with a series of wavelengths of the transmission dip were obtained by adjusting the anodization voltage, and all the intensities of the transmission dip were kept at a low value. A redshift of the transmission dip is found for the increasing anodization voltage. The diffraction is similar to X-ray diffraction and optical reflection spectra in thin film. The following equation should be considered

$$2d(n_2^2 - n_1^2 \sin^2 \theta)^{1/2} = m\lambda \qquad [1]$$

where n_2 and n_1 are the average refractive indexes of the alumina membrane and air, respectively, θ is the incidence angle, and d is the distance between the branched channels, as shown in Fig. 1c and 2. λ is the wavelength of the diffracted light in air, usually characterized by the minimum in transmission or maximum in reflectance spectra. m is an order of diffraction, and the transmission dips in samples 1#–7# represent the first order of the diffraction. It is supposed that the thickness of the film is proportional to the integral of current density to time

[z] E-mail: huxing@scut.edu.cn

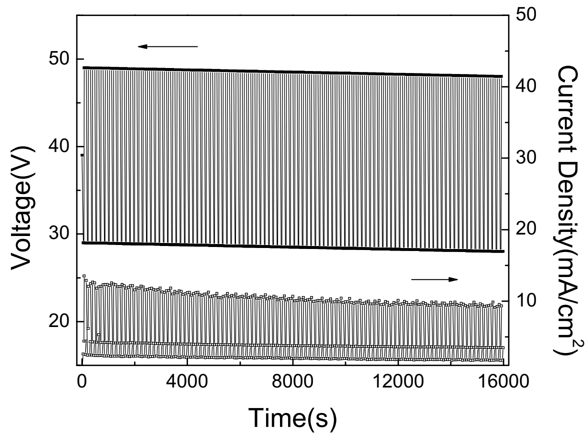

(a)

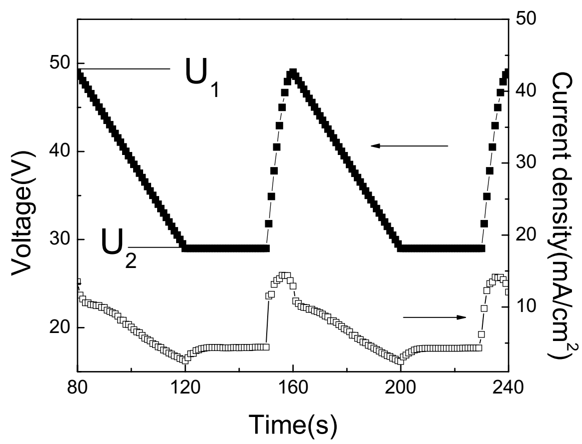

(b)

(c)

Figure 1. Curves of (a) the periodic cell voltage time and current density time and (b) the enlarged part; (c) illustrations of the main channel and the branched channel in a photonic crystal of anodic alumina.

$$Q = \int idt \qquad [2]$$

where Q is the charge passed during time (Δt) and i is the current density at time (t). The distance between the branched channels is proportional to the current density and time. The wavelength of the dips increases with the increasing benchmark anodic voltage shown in Fig. 3b because of the increasing distance between the branched channels (Fig. 2), which could be reflected by the current density (not shown).[12]

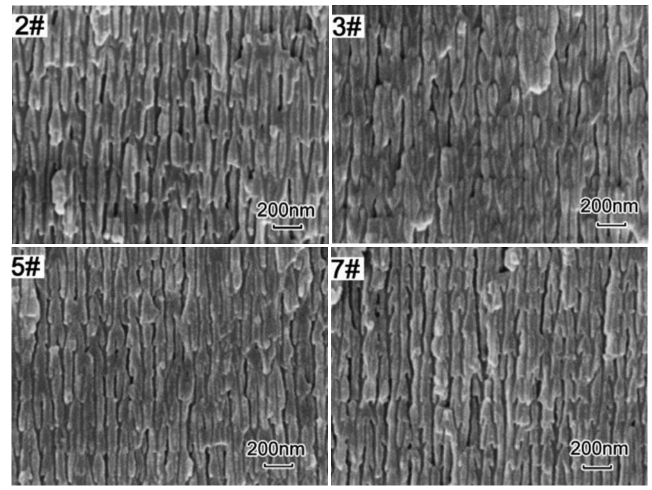

Figure 2. The cross-sectional scanning electron microscopy images of the alumina membrane (the middle of the fracture surface).

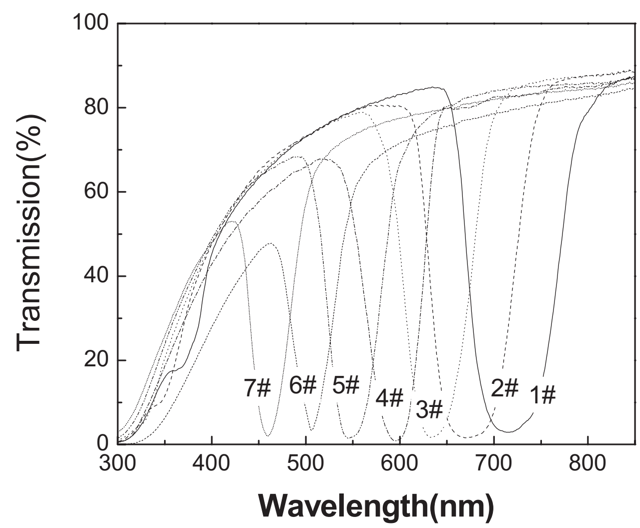

(a)

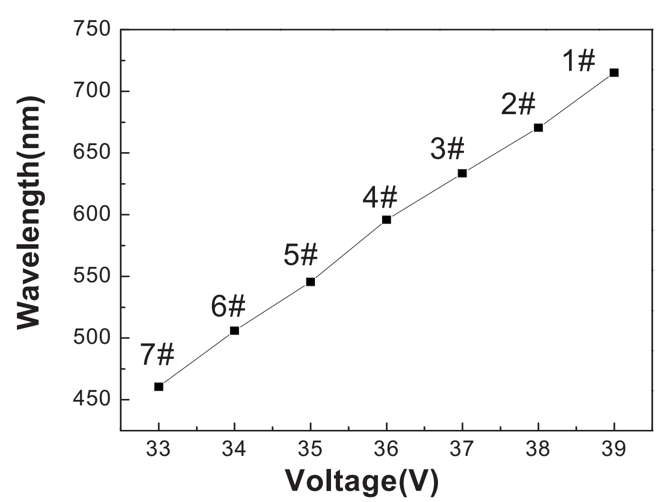

(b)

Figure 3. (a) Tuning optical transmission spectra of the anodic alumina; (b) the wavelength of transmission dip as the function of the initial benchmark anodic voltage.

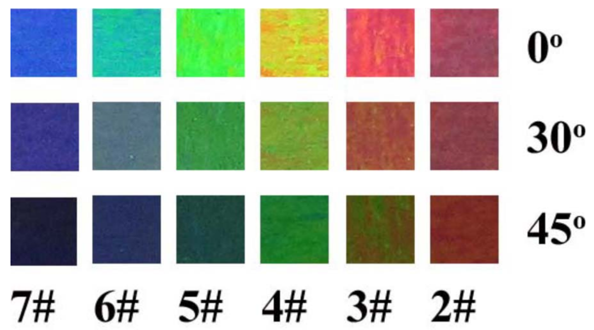

(a)

(b)

Figure 4. (Color online) Photographs of photonic crystal (a) with black background at different observable angle (reflection angle) and (b) with Al substrate.

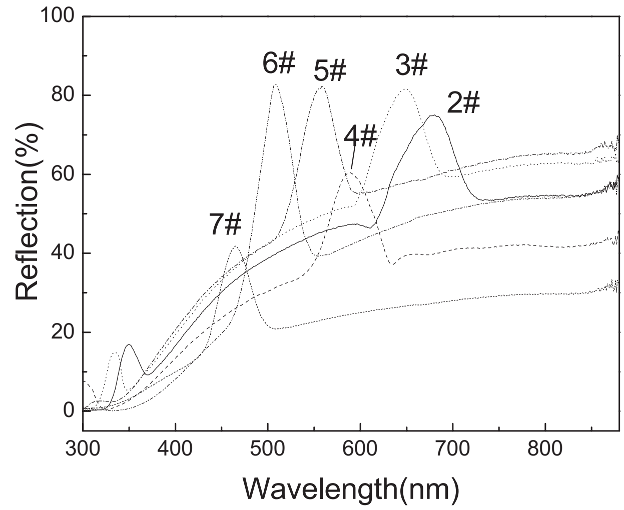

(a)

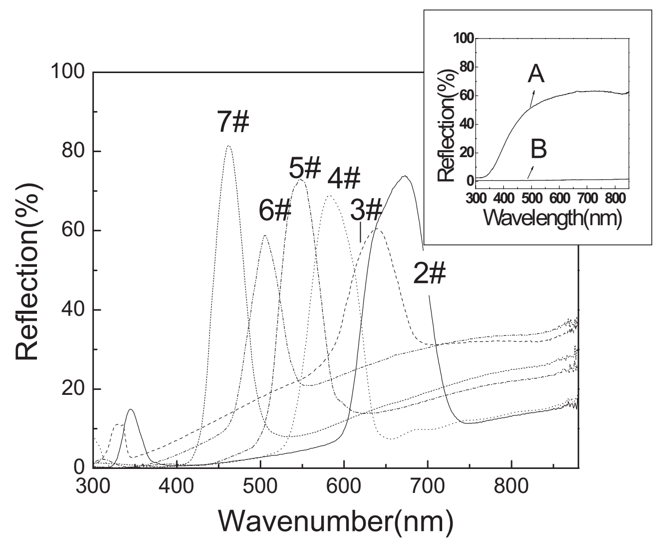

(b)

Figure 5. Optical reflection spectra of (a) photonic crystal with Al substrate and (b) electrodeposited photonic crystal with Al substrate [The inset shows the reflection spectra of general porous alumina with Al substrate (A) without electrodeposition and (B) with electrodeposition].

The photographs of the photonic crystal with a black background are shown in Fig. 4a. The anodic alumina with the color from blue (7#) to red (2#) is obtained. The color of photonic crystal is strongly dependent on the observable angle, and the blueshift in color is reasonably well described by Bragg's law,[13] as shown in Fig. 4a. Though the vivid color is observed for the photonic crystal with a black background, the color of the photonic crystal with an Al substrate is not visible, as shown in Fig. 4b. In chroma theory,[14] the incorporation of white light decreases the purity of the color. As shown in Fig. 5a, the reflection spectra of the porous alumina with an Al substrate include the diffraction of the porous alumina and the reflection from the alumina film/Al interface. The strong reflection from the Al substrate results in invisible color of the photonic crystal.

To color the photonic crystal with Al substrate, the reflection from Al has to be suppressed and the diffraction from the photonic crystal should not be affected. An effective way is to introduce an absorption layer at the bottom of the anodic alumina. To absorb the light, nickel is always used for the black coloring process, as in thermal energy production from solar energy.[15] In the present work, tin/nickel is used for the deposition in the porous alumina.[16] With enough deposition time, the reflection from Al substrate can be suppressed seriously. The black was obtained in the general porous alumina template, as shown in the inset of Fig. 5b. The discussion on the details of the deposition is beyond the scope of the present paper.

As shown in Fig. 5b, after the deposition, the intensity of reflection from the Al substrate is reduced by more than 30% compared with that before deposition. It indicates a strong absorption for the deposited Sn/Ni layer. The difference in the intensity of the reflection peak between Fig. 5a and b may be from a discrepancy in the samples such as a contamination or bend. The photographs of photonic crystal with electrodeposited metal having tuned optical properties are shown in Fig. 6a. After deposition, the color evolved from blue to red in the photonic crystal with Al substrate. The difference between Fig. 4a and 6a is possibly from the resident light reflection from the Al substrate, as shown in Fig. 5b. It also indicates that the color could be tuned by adjusting the reflection from the Al substrate, which is controlled by the deposition time. As shown in Fig. 6a, with the increasing observable angle, the color of the photonic crystal could change from blue to black or from black to red (not shown) obeying the Bragg law.

The sketch map of the optical processes is also illustrated in Fig. 6b. When the light beam is incident on the anodic alumina, the light obeying the Bragg law is reflected; the remaining beam is attenuated during propagation through the deposition layer; the beam passed through the deposition layer is reflected on the interface and then suppressed seriously when passing through the deposition layer again; all the light attenuates when propagating through the alumina for the absorption and scattering; the light reflects on the interface of air/alumina and air/deposition, but it could be neglected. Finally, the emission light from the photonic crystal includes the diffraction light and the fading reflection light from Al substrate.

Conclusions

In the present paper, the tuning of optical properties in photonic crystal of anodic alumina was obtained by adjusting the anodization voltage, and the aluminum was colored for photonic crystal with metal electrodeposition. The transmission spectra of photonic crystal show the redshift of the reflection peak with the increasing anodic voltage and the blueshift of the color with observable angles corresponding to the Bragg law. The variation in the optical properties of

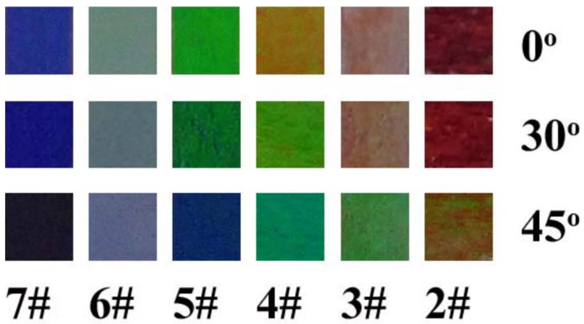

(a)

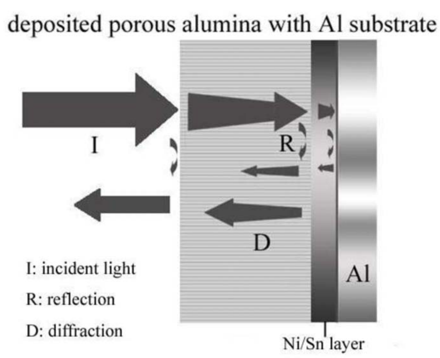

(b)

Figure 6. (Color online) (a) Photographs of photonic crystal from the electrodeposition with Al substrate and (b) sketch map of optical processes.

photonic crystal with the variation in periodic anodizing is due to the variation in the distance between the branched channels. The electrodeposited metal layer strongly absorbs the reflecting light from the Al substrate, and it makes the photonic crystals with an Al substrate show vivid colors. It is expected that the present process can open up an area for the industrial application of photonic crystals.

Acknowledgment

This work was supported by the Scientific Research Foundation for the Returned Overseas Chinese Scholars, State Education Ministry and the Scientific and Technological Planning Project of Guangdong Province (no. 2007A010500012).

South China University of Technology assisted in meeting the publication costs of this article.

References

1. M. Campbell, D. N. Sharp, M. T. Harrison, R. G. Denning, and A. J. Turberfield, *Nature (London)*, **404**, 53 (2000).
2. D. L. Guo, L. X. Fan, F. H. Wang, S. Y. Huang, and X. W. Zou, *J. Phys. Chem. C*, **112**, 17952 (2008).
3. D. J. Norris, E. G. Arlinghaus, L. Meng, R. Heiny, and L. E. Scriven, *Adv. Mater.*, **16**, 1393 (2004).
4. U. Grüning, V. Lehmann, and C. M. Engelhardt, *Appl. Phys. Lett.*, **66**, 3254 (1995).
5. H. Masuda, M. Ohya, H. Asoh, M. Nakao, M. Nohtomi, and T. Tamamura, *Jpn. J. Appl. Phys., Part 2*, **38**, L1403 (1999).
6. B. Wang, G. T. Fei, M. Wang, M. G. Kong, and L. D. Zhang, *Nanotechnology*, **18**, 365601 (2007).
7. W. Lee, K. Schwirn, M. Steinhart, E. Pippel, R. Scholz, and U. Gösele, *Nat. Nanotechnol.*, **3**, 234 (2008).
8. D. Losic and D. Losic, *Langmuir*, **25**, 5426 (2009).
9. H. J. Gohausen and G. C. Schoener, *Plat. Surf. Finish.*, **2**, 56 (1984).
10. H. M. Chen, C. F. Hsin, R. S. Liu, S. F. Hu, and C. Y. Huang, *J. Electrochem. Soc.*, **154**, K11 (2007).
11. W. J. Zheng, G. T. Fei, B. Wang, and L. D. Zhang, *Nanoscale Res. Lett.*, **4**, 665 (2009).
12. X. Hu, Z. Y. Ling, X. H. He, and S. S. Chen, *J. Electrochem. Soc.*, **156**, C176 (2009).
13. X. Hu, Z. Y. Ling, S. S. Chen, and X. H. He, *Chin. Phys. Lett.*, **25**, 3284 (2008).
14. G. Wyszecki and W. S. Stiles, *Color Science: Concepts and Methods, Quantitative Data and Formula*, Wiley, New York (1982).
15. L. Anicai, A. Pertache, and T. Visan, *Surf. Interface Anal.*, **40**, 818 (2008).
16. S. Kawai, *Anodizing and Coloring of Aluminum Alloys*, ASM International, Materials Park, OH (2002).